THE AMERICAN SOCIETY OF MECHANICAL ENGINEERS
345 E. 47 St., New York, N.Y. 10017

86-GT-244

The Society shall not be responsible for statements or opinions advanced in papers or in discussion at meetings of the Society or of its Divisions or Sections, or printed in its publications. Discussion is printed only if the paper is published in an ASME Journal. Papers are available from ASME for fifteen months after the meeting.
Printed in USA.

Copyright © 1986 by ASME

The Development of the Profile Boundary Layer in a Turbine Environment

J. HOURMOUZIADIS, F. BUCKL, P. BERGMANN
Turbine Aerodynamics
MTU Motoren- und Turbinen-Union München GmbH
Dachauer Str. 665
8000 München 50

ABSTRACT

Cascade testing tries to simulate the actual flow conditions encountered in a turbine. However, it is neither possible to reproduce the free stream turbulence structure of the turbomachinery, nor the periodic wake effects of upstream blade rows. The usual understanding is that the latter in particular results in a significantly different behaviour of the boundary layer in the engine.

Experimental results from cascades and turbine rigs are presented. Grid generated free stream turbulence structure is compared to that in the turbine. Measurements of the profile pressure distribution, flush mounted hot films and flow visualization were used for the interpretation of the test results. Some observations of the boundary layer development in the cascade, on the guide vanes and on rotor blades with typically skewed boundary layers are shown indicating essentially similar behaviour in all cases.

NOMENCLATURE

d	m	diameter, trailing edge thickness
e	V	RMS hot film signal
E	V	time average hot film signal
E_o	V	time average hot film signal at zero flow
f	Hz	frequency
F	Hz	frequency range
L	m	length scale of velocity fluctuations
P_t	Pa	total pressure
M	-	Mach number
Re	-	Reynolds number
s	m	curved coordinate of the profile surface
Sr	-	Strouhal number
t	m	cascade pitch
u	m/s	velocity in the shear layer
u'	m/s	velocity fluctuation
U	m/s	main flow velocity
V	m/s	eddy convection velocity
α	1/m	wave number
β	-	Hartree parameter
δ_1	m	displacement thickness
η	kg/(m s)	dyn. viscosity
λ	-	relative length scale of velocity fluctuations
τ	Pa	shear stress

SUBSCRIPTS

I	integral value
F	frequency range
w	wall

INTRODUCTION

The overall performance of a turbine depends primarily on the viscous effects in the flow. This is particularly true for turbines in aircraft engines where large portions of the boundary layer on the airfoils are laminar. In this case early laminar/turbulent transition would increase turbulent friction losses, late transition would tend to increase sensitivity to laminar separation, both leading to performance deterioration. In cooled turbines these phenomena would also have influence on heat transfer to the blade and may penalize life. Evidently close control of transition is necessary to hold and improve on the present high levels of performance.

It is well known that turbulence can have a strong effect on the transition of shear layers. This has been accepted for some time and extensive experimental work has been carried out to determine the influence of the degree of turbulence on cascade performance. Reviews have been presented by J. Surugue /1/ and R. Kiock /2/. Adapting the point of view of fundamental boundary layer research, in many cases devices have been used to produce isotropic or at least uniform turbulence at the entry to the test section. This permits a clear separation of turbulence from other effects. Unfortunately, the situation in turbomachinery is more complicated. The turbulence produced in wakes usually does not have sufficient time to become uniform before it interacts with the boundary layer of the next row. The wakes of rotating blades produce discrete frequency fluctuations for the stationary vanes. Changing from the absolute to the relative frame and vice versa directly effects the components of velocity fluctuations. Finally the problem is further complicated by radial movement of the fluid in secondary flows.

To reduce complexity, modelling of these phenomena at the present has to remain essentially 2-dimensional. Nevertheless, it is quite obvious that the degree of turbulence, alone, is not sufficient to describe the flow. It is necessary to include some more sophisticated considerations of the makroskopic structure of turbulence. These could help to separate for example the following different forms of interaction with a shear layer:

Presented at the International Gas Turbine Conference and Exhibit
Dusseldorf, West Germany—June 8-12, 1986

Downloaded from http://asmedigitalcollection.asme.org/GT/proceedings-pdf/GT1986/79283/V001T01A107/2396574/v001t01a107-86-gt-244.pdf by guest on 16 August 2022

- Very slow fluctuations (very large eddy) representing quasi steady state flow for the boundary layer.
- Slow fluctuations producing true unsteady flow, as in the experiments of D.J. Doorly and M.L.G. Oldfield /3/.
- Fast fluctuations in the unstable region of the laminar boundary layer initiating transition. These are either introduced into the flow with isotropic turbulence, or with periodic wakes as in the experiments of H. Pfeil and R. Herbst /4/, or with discrete frequency excitation as for example reported by Yu.S. Kachanov and V.Ya. Levchenko /5/.
- Very fast fluctuations (very small eddy) which are damped away in the boundary layer and have no effects.

To resolve these phenomena some more detailed information about the turbulence environment in a turbine is required. Measurements in a variety of turbine rigs are presented in this paper, and the characteristics are compared to grid generated turbulence. The observed behaviour of the 2-dimensional profile boundary layer in such an environment is shown for guide vanes and rotor blades using different measurement techniques.

EXPERIMENTAL FACILITIES

Turbulence measurements were carried out in three different turbine rigs and behind grids placed in a jet flow. The experiments with the profile boundary layer were carried out in two of the turbine rigs.

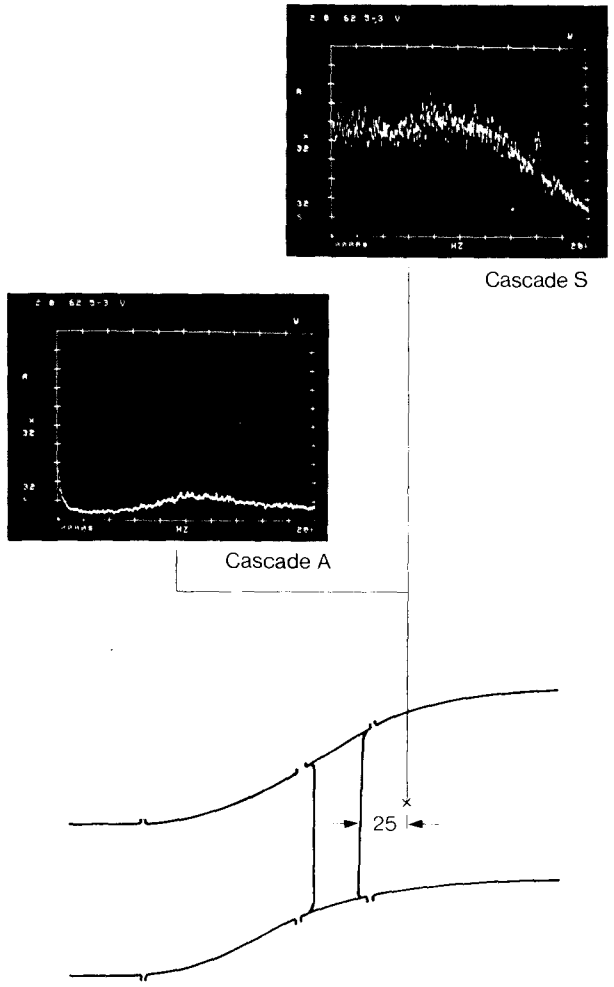

Fig. 1 ANNULAR CASCADE RIG AND TYPICAL FREQUENCY SPECTRA OF TURBULENCE FOR CASCADES A AND S

Fig. 1 shows the annular cascade rig for the first guide vane of a low pressure turbine. Very extensive aerodynamic measurements were carried out in this set up with two different cascades. This included static taps and flow visualization on the airfoil and circumferential traversing of the flow 25 mm downstream of the trailing edge at the mean section both with a five hole pressure probe and a hot wire probe.

In the two stage rig shown in Fig. 2 the measurements concentrated on the profile boundary layer of the guide vanes using static taps and hot films at the mean section. Flow visualization was applied both on guide vanes and rotor blades. Turbulence measurements could be done 395 mm downstream of the trailing edge of the second rotor only. A hot film cylinder probe was used. The first guide vane was one of the annular cascades used in the rig of Fig. 1.

The third rig, a single stage high pressure turbine, is shown in Fig. 3. Turbulence measurements were conducted 5 mm downstream of the rotor trailing edge at the 3 o'clock position and 40 mm at the 1 o'clock position at the mean section. No traversing was done. A hot film cylinder probe was used for these tests.

The experiments with the turbulence grids were carried out in the jet behind a nozzle of 100 mm diameter shown in Fig. 4. The grids were mounted on the nozzle. Bar diameter/mesh width was 0.3/1.0; 0.8/3.3; 6/19 and 8/20 mm. Both hot wire and hot film cylinder probes were used.

The turbine parts were genuine engine hardware. For the turbulence measurements DISA probes were used. The flush mounted hot films for the boundary layer investigations were developed and manufactured at MTU. Development and calibration techniques will be reported by P. Pucher and R. Göhl /7/. A TSI 1050 CTA anemometer was used for the tests. The signals were taken on tape and were further processed with a NICOLET 446B FFT real time analyzer.

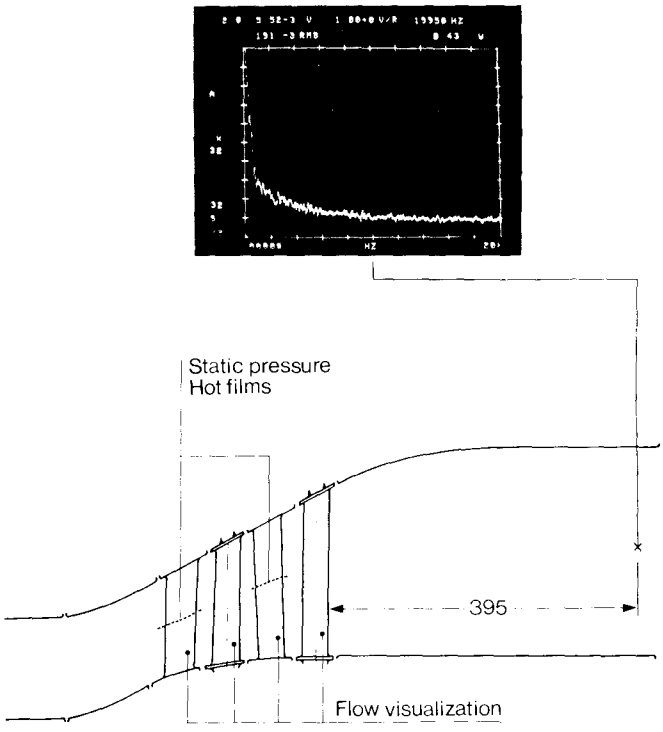

Fig. 2 TWO STAGE LP TURBINE RIG AND TYPICAL FREQUENCY SPECTRA OF TURBULENCE

Downloaded from http://asmedigitalcollection.asme.org/GT/proceedings-pdf/GT1986/79283/V001T01A107/2396574/v001t01a107-86-gt-244.pdf by guest on 16 August 2022

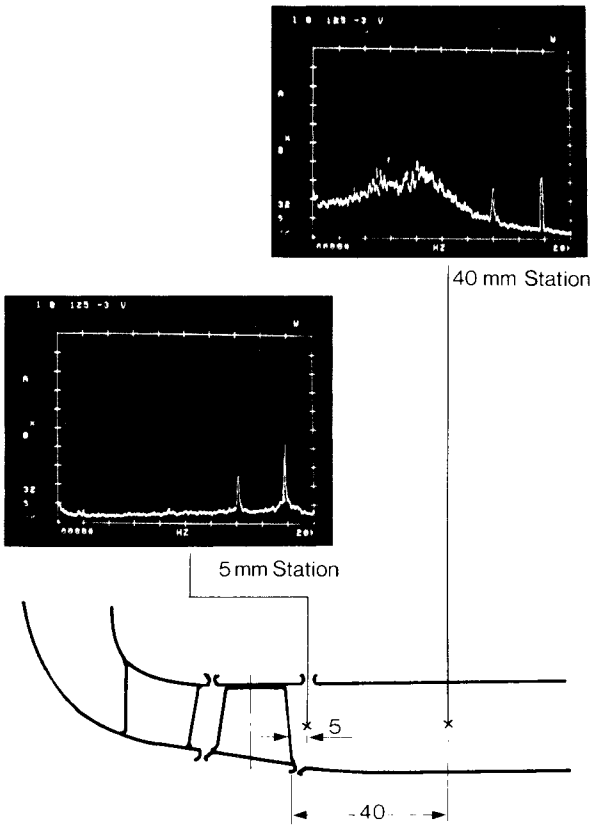

Fig. 3 HP TURBINE RIG AND TYPICAL FREQUENCY SPECTRA OF TURBULENCE

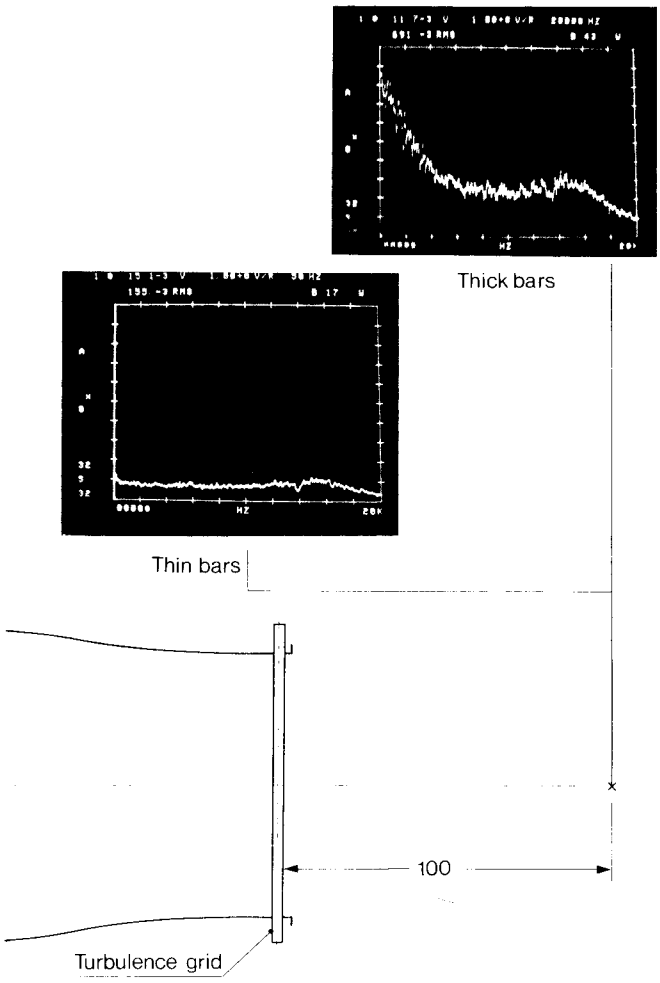

Fig. 4 NOZZLE WITH TURBULENCE GRIDS AND TYPICAL FREQUENCY SPECTRA OF TURBULENCE

THE MAKROSTRUCTURE OF TURBULENT FLUCTUATIONS

For the classification of the interaction between turbulence and a shear layer the size of the eddies has been used in the introduction indicating the necessity for a characteristic length. Originally it was G.I. Taylor /6/ who presented an analysis of turbulence in 1936 suggesting that not only the amplitude but also the wave length of the disturbance are the two important parameters. Stability theory for laminar flow uses only the wave length. Frequency spectra can indeed show quite different qualities. In the case of Fig. 2 the amplitude is practically independent of the frequency except for very low values. In the case of Fig. 3 at the 40 mm downstream station, turbulence appears to be rather strong around 4 kHz falling off at lower and higher frequencies. Additionally strong fluctuations can be observed at the discrete frequencies of 14 and 18 kHz. It should be expected that a shear layer would react differently to these two disturbances.

The individual disturbance can be described using its characteristic frequency f. The disturbance is convected downstream with the velocity V. This velocity can be used to define a length scale L

$$L = \frac{V}{2 \pi f} \qquad (1)$$

In terms of the eddy model this is the wave length of the fluctuation. In free shear layers V is assumed to be equal to the local mean velocity of the flow U

$$V = U \qquad (2)$$

These definitions can be directly applied to discrete frequency disturbances. For random fluctuations, however, integral scales have to be introduced. An integral frequency $f_{I,F}$ can be defined by an amplitude weighted averaging process over the frequency range of 0 to F kHz

$$f_{I,F} = \frac{\int_0^F f \sqrt{\overline{u'^2}}\, df}{\int_0^F \sqrt{\overline{u'^2}}\, df} \qquad (3)$$

Accordingly the integral length scale is

$$L_{I,F} = \frac{V}{2 \pi f_{I,F}} \qquad (4)$$

For uniform turbulence, where the amplitude is constant, the integral frequency can be readily calculated to be equal to F/2. An integral frequency value below F/2 indicates that the slower fluctuations are more pronounced, a value above F/2 means that the higher frequencies are dominating. This suggests the introduction of relative parameters like the relative integral length λ

$$\lambda_{I,F} = \frac{L_{I,F}}{L_{I,F\ \text{uniform}}} \qquad (5)$$

Downloaded from http://asmedigitalcollection.asme.org/GT/proceedings-pdf/GT1986/79283/V001T01A107/2396574/v001t01a107-86-gt-244.pdf by guest on 16 August 2022

With equation (4) this gives

$$\lambda_{I,F} = \frac{f_{I,F\ uniform}}{f_{I,F}} = \frac{F/2}{f_{I,F}} \qquad (6)$$

It should be noted that these parameters are still integral values just the same as the degree of turbulence. $\lambda_{I,F} = 1$ does not imply the existence of uniform turbulence. It only indicates that overall turbulence levels below and above F/2 are equal, whatever the distribution in these two regions may look like. Nevertheless, the integral length is besides the degree of turbulence the second independent parameter which is necessary to describe the overall characteristics of amplitude and frequency.

In general these considerations have to be applied to the three possible directions of the fluctuations. However these are seldom available from measurements in turbomachinery. Results reported here include the streamwise and radial fluctuation. The frequency range has been limited to 20 kHz. This is somewhat low for hot wire probes, but the experimental set up and other probes used, tend to make measurements beyond that unreliable. Unless indicated otherwise, integral values in this study do not include discrete frequency amplitudes.

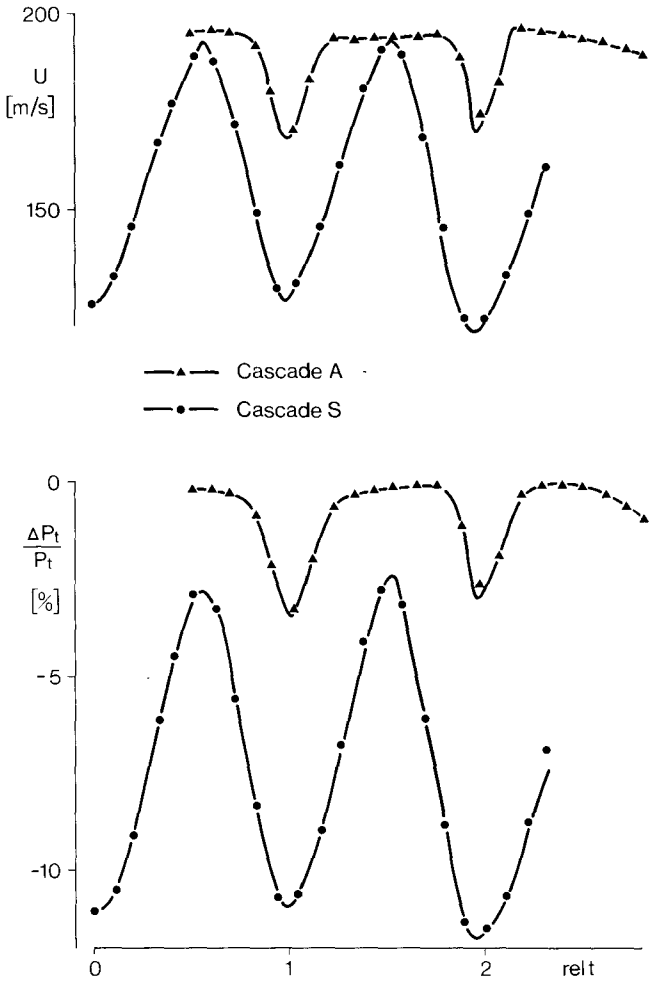

Fig. 5 VELOCITY AND TOTAL PRESSURE LOSS DISTRIBUTION DOWNSTREAM OF THE ANNULAR CASCADES A AND S

TURBULENCE MEASUREMENT RESULTS

The most conclusive results were obtained with the annular cascade rig shown in Fig. 1, because one of the cascades investigated showed non-reattaching laminar separation. Test conditions were adjusted to give a Reynolds number of 200000 defined with exit parameters and true chord.

The flow parameters were traversed tangentially 2.5 times the pitch in width. Fig. 5 shows the velocity U and total pressure loss $\Delta P_t/P_t$ wakes over the relative pitch. Fig. 6 shows the overall degree of turbulence Tu and the relative integral length scale $\lambda_{I,20}$. The phase shift between the two cascades is arbitrary.

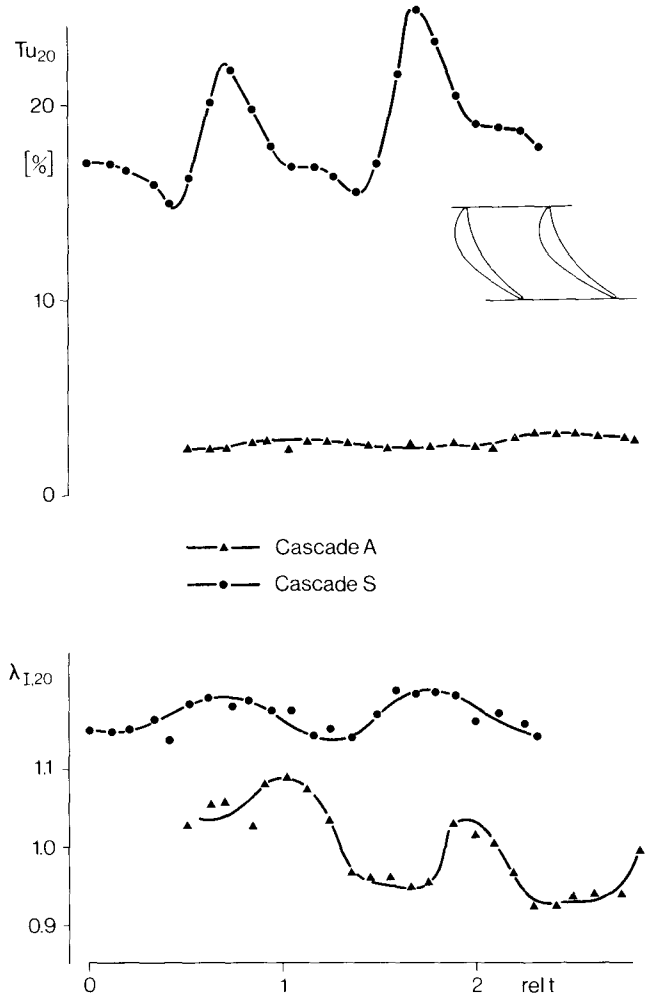

Fig. 6 DEGREE OF TURBULENCE AND RELATIVE INTEGRAL LENGTH DOWNSTREAM OF THE ANNULAR CASCADES A AND S

The total pressure losses increased dramatically from cascade A to cascade S, very similar to the transonic tests of O. Lawaczeck /8/ where the phenomenon was also caused by separation. The presence of laminar separation on cascade S was confirmed by the profile static pressure distribution and flow visualization, which also showed that on cascade A the boundary layer remained attached up to the trailing edge.

The measurement station is about one axial chord downstream of the vane row where significant mixing should already have taken place. However, the velocity deficit in the wake of cascade A is still 13% and 34% for cascade S.

Downloaded from http://asmedigitalcollection.asme.org/GT/proceedings-pdf/GT1986/79283/V001T01A107/2396574/v001t01a107-86-gt-244.pdf by guest on 16 August 2022

Velocity gradients are practically the same for both cases.

Much more interesting are the turbulence wakes. Although velocity gradients still exist, cascade A shows a constant degree of turbulence below 2% with relative integral length scales in the vicinity of 1. This confirms the observation of R. Kiock /9/ that the dissipation of turbulence is significantly faster than the decay of the mean velocity wake. He reported on similar levels of turbulence at the same distance from the trailing edge downstream of a compressor cascade.

O.P. Sharma, T.L. Butler, H.D. Joslyn and R.P. Dring /10/ obtained 8% maximum degree of turbulence 0.1 axial chords downstream of the inlet guide vane of a 1 1/2 stage low velocity rig turbine. Taking the dissipation rate into account, this is also comparable to the present results.

The separated flow of cascade S shows levels of turbulence one order of magnitude higher and relative length scales of about 1.2. The latter indicates that lower frequencies dominate as can also be seen from the RMS spectra in Fig. 1. The velocity gradients present in this station would not indicate sufficient turbulence production to explain these values. They are probably due to turbulence produced closer to the cascade where the suction side main flow mixes at the free shear layer with the dead water of the separation zone. In that region the highest velocity gradients in the flow are present. This is in agreement with the distribution of turbulence. The highest levels can be observed on the suction side leg of the wake quite close to the edge of the mixing zone. R. Kiock /11/ identified a similar behaviour of turbulence in a compressor. It was attributed to laminar separation which developed when Reynolds numbers were reduced below a critical value.

The RMS spectra of Fig. 1 show a strong amplitude at 16 kHz for cascade S which could not be explained by any frequency of the system and which was not observed in cascade A. Assuming a Strouhal number Sr = 0.2 for the wake of a body with a displacement diameter d

$$Sr = \frac{f\,d}{U} \qquad (7)$$

a value of d = 2.4 mm can be calculated. This is approximately the predicted total displacement effect of pressure side boundary layer, trailing edge thickness, suction side separation zone and suction side free shear layer, implying the presence of a vortex wake. The corresponding frequency for cascade A was expected to be beyond the range of the measurements. It could still be identified at 28 kHz, giving about half the displacement effect of cascade S. In both cases the amplitude of the signal had a peak in the core of the wake. If these observations can be verified they would present a rather simple method of identifying flow separation in turbine cascades.

From the results of these tests two facts should be pointed out:

- High levels of turbulence in turbines can be produced in the mixing out of separation zones and not only by the periodic wakes between stationary and rotating blade rows.
- The measuring station lies within the blade passage of the downstream rotor of the complete stage shown in Fig. 2. It is obvious that turbulence there would by no means have to be uniform. In the case of cascade S for example the rather complex structure shown in Fig. 1 including periodic disturbances would be present.

The integral parameters, degree of turbulence and relative length scales are shown in Fig. 7. The periodic vortex wake has been separated from the random turbulence for cascade S. It is shown at low levels of relative length scale and degree of turbulence.

Test results of the two stage rig Fig. 2 are also plotted in the diagram. Turbulence measurements only far downstream were possible in this experiment. Rotor speed was varied between 80% and 120% and first vane Reynolds number between

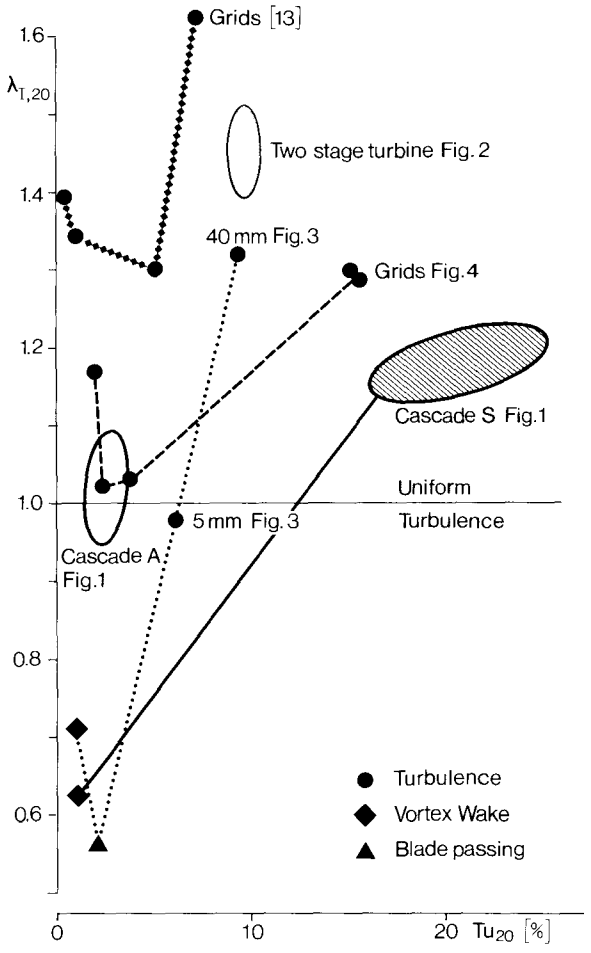

Fig. 7 INTEGRAL CHARACTERISTICS OF TURBULENCE IN TURBINES AND BEHIND GRIDS

160000 and 480000. In all cases the frequency spectra look very similar to that shown in Fig. 2. The distribution is practically constant except for very low frequencies. Obviously the measuring station about 15 axial chords away from the last row is so far downstream that the different operating conditions have no effect. Even the blade passing frequencies do not show. Relative integral length scales are between 1.4 and 1.5, turbulence levels are about 10%, which is partly due to the mean velocity reduction in the diffusing annulus of the test rig.

Typical spectra for the high pressure turbine rig are shown in Fig. 3. Surprisingly, the station 5 mm downstream of the rotor shows a more uniform distribution than the 40 mm downstream station. The blade passing frequency can be readily identified for both stations. Also in both stations a periodic signal can be observed at 14 kHz. After transformation to the relative frame this could be attributed to the vortex wake of the rotor blades. Both discrete frequency signals appear at the very low length scale region of Fig. 7.

The overall degree of turbulence was found to be between 6% and 9% in both stations, the lower value corresponding to integral length scales of 1.0, the higher to 1.3. Laser velocimeter measurements 3 mm downstream of the trailing edge triggered to a fixed blade to vane position gave values of 8% to 16% along the guide vane pitch.

Downloaded from http://asmedigitalcollection.asme.org/GT/proceedings-pdf/GT1986/79283/V001T01A107/2396574/v001t01a107-86-gt-244.pdf by guest on 16 August 2022

This sums up the available data on turbulence structure in turbines. It covers a range of Tu = 2% to 25% and $\lambda_{I,20}$ = .95 to 1.50. Periodic fluctuations lie about Tu = 2% and $\lambda_{I,20}$ = 0.5 to 0.6. Because of the limited data base, this does not cover the whole range to be encountered in a gas turbine. It should also be noted that this data only includes cold rig experiments. Applying Mach number similarity, blade passing frequencies for example would be about two times higher in a hot engine environment.

For comparison grid generated turbulence is also shown in Fig. 7. Results from the free jet tests of Fig. 4 give for bar diameters below 0.8 mm values close to uniform turbulence with $\lambda_{I,20}$ = 1 and Tu = 2% to 4%. The thicker bars give both higher levels of turbulence and length scales. The differences can be easily understood when the spectra in Fig. 5 are compared. In the case of the thicker bars, the distance of the measuring station 100 mm downstream of grids did not fulfill the criterion given by M.F. Blair /12/ of ten mesh lengths for uniform turbulence.

Further data are included from measurements in a high velocity cascade test facility by R. Kiock, G. Laskowski and H. Hoheisel /13/. Degrees of turbulence up to 8% with length scales between 1.3 and 1.6 were achieved.

The data collected in Fig. 7 shows that grid generated turbulence is quite similar to that found in turbomachinery as far as overall parameters are concerned. One should not be afraid to put the grids close to the test section. The irregularities appearing there look much like those found in a turbine. Periodic disturbances will have to be introduced separately into the flow.

BOUNDARY LAYER INVESTIGATION

Because of the fundamental importance of the turbulence intensity and turbulence structure to the boundary layer development, boundary layer experiments were carried out with the two stage rig shown in Fig. 2. The Reynolds number was set at 200000 for the first guide vane. As mentioned before, genuine engine parts were used. The measurement techniques applied were:

- Static pressure taps around the profile at the mean section on both guide vanes.
- Hot film probes on the suction side at the mean section on both vanes.
- Flow visualization on all four rows.

The purpose of the test was to identify the state of the boundary layer along the suction surface and localize transition. The boundary layer behaviour of the four rows should be compared in terms of the effects of periodic disturbances from the wakes of the upstream rows.

Fig. 8a shows for the first vane the Mach number distribution, calculated from static to inlet total pressure, over the normalized curved coordinate s of the profile surface. The transition of the separated laminar boundary layer with following turbulent reattachment can be clearly seen on the diffusing part of the suction side. This is in good agreement with the boundary layer prediction.

The time average hot film signal E, corrected for the zero flow effect E_0, is plotted on Fig. 8b. For ideal conditions, with no heat transfer from the probe at zero flow, this signal is proportional to $\tau_W^{1/6}$.

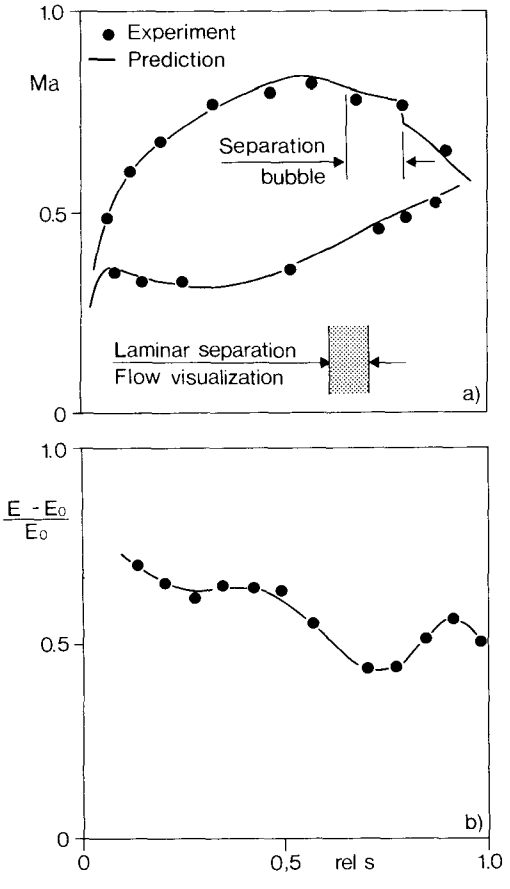

Fig. 8 MACH NUMBER DISTRIBUTION AND TIME AVERAGE HOT FILM SIGNAL FOR THE FIRST GUIDE VANE OF THE TWO STAGE RIG AT THE MEAN SECTION

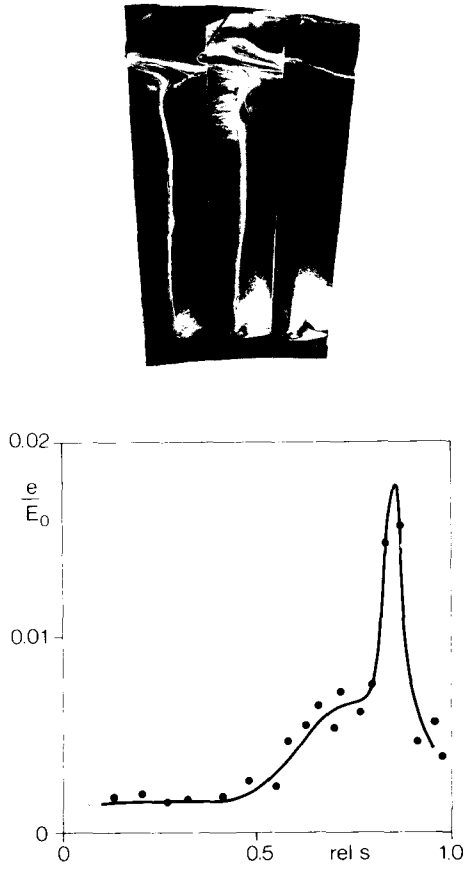

Fig. 9 TOTAL RMS HOT FILM SIGNAL AND FLOW VISUALIZATION FOR THE FIRST GUIDE VANE OF THE TWO STAGE RIG AT THE MEAN SECTION

Downloaded from http://asmedigitalcollection.asme.org/GT/proceedings-pdf/GT1986/79283/V001T01A107/2396574/v001t01a107-86-gt-244.pdf by guest on 16 August 2022

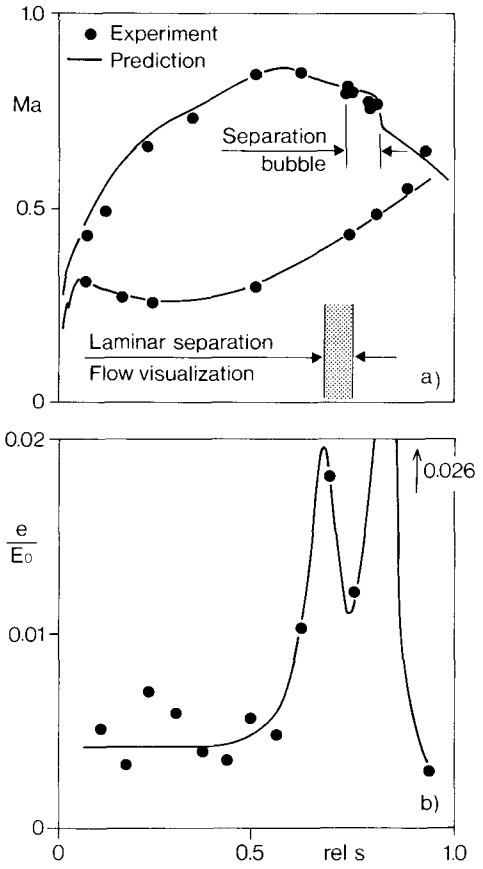

Fig. 10 MACH NUMBER DISTRIBUTION AND TOTAL RMS HOT FILM SIGNAL FOR THE SECOND GUIDE VANE OF THE TWO STAGE RIG AT THE MEAN SECTION

Unfortunately the heat loss to the vanes is usually much greater than the heat transfer due to the shear stress. Only with a very difficult calibration procedure it would be possible to calculate wall shear stress from the hot film results, as H.P. Hodson /14/ did for his tests. Nevertheless very good relative information can be extracted from the signal. In Fig. 8b high values of E can be identified in the region of acceleration, because of the thin boundary layer and the high wall shear stress. A minimum is expected at the separation point with zero wall shear stress. It can be found at the same position where the separation bubble was identified from the Mach number distribution. Further downstream the signal is higher, which can be explained by reattachment.

The fluctuating signal e of the hot film probes is plotted in Fig. 9. The RMS value is normalized with E_0. A very pronounced maximum can be observed. It corresponds exactly to the point of turbulent reattachment. The curve also shows a disturbance further upstream, which is close to the laminar separation point. These phenomena are discussed in more detail later.

For flow visualization, liquid dye was injected into the flow through static pressure taps during operation. The results, also shown in Fig. 9, confirm the conclusions about the transition process. The laminar separation can be clearly identified. The radial pressure gradients accelerate the stagnating fluid within the bubble towards the hub. A very clear picture of the dead water zone is drawn, very similar to that obtained by H.E. Rohlik, H.W. Allen and H.Z. Herzig /15/ in 1953.

Contrary to the situation with the first guide vane, the second is directly affected by the wakes of the upstream rotor. The Mach number distribution and the RMS signal of the hot film probes for this vane are shown in Fig. 10. Static pressure taps were spaced too far apart in this case to identify a separation, the boundary layer prediction however did show a small bubble on the suction side. This could be confirmed again both by the hot film measurements and the flow visualization. The RMS signal shows in this case two very pronounced maxima. One at the laminar separation and the other at the turbulent reattachment point.

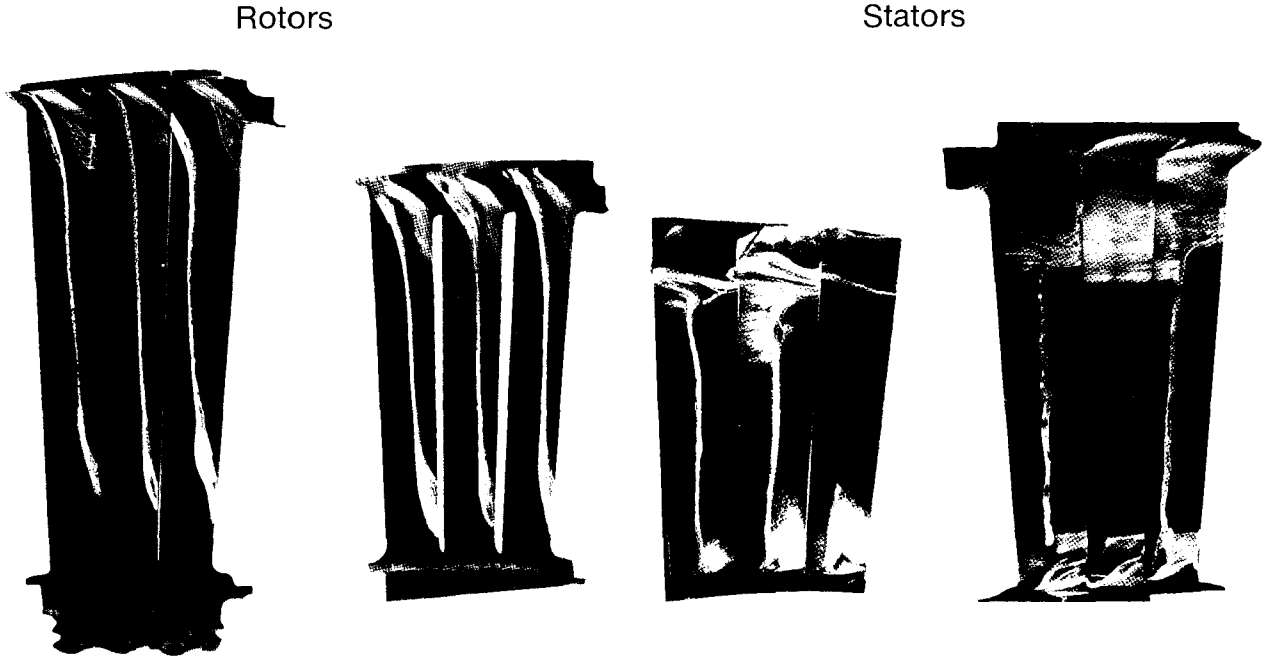

Fig. 11 FLOW VISUALIZATION ON THE SUCTION SIDE OF GUIDE VANES AND ROTOR BLADES

Downloaded from http://asmedigitalcollection.asme.org/GT/proceedings-pdf/GT1986/79283/V001T01A107/2396574/v001t01a107-86-gt-244.pdf by guest on 16 August 2022

The former obviously corresponds to the disturbance which was also observed on the first guide vane. The difference can be explained in fact by the presence of the rotor wakes in the second vane.

Comparing the two airfoils, the separation seems to be larger on the first vane. One might tend to attribute this to the abscence of the upstream rotor. However the boundary layer prediction indicates that this could also be caused by the different pressure distributions alone.

A similar situation with the wakes of the guide vanes is given for the rotor airfoils. Furthermore the boundary layer on the rotating blades is nowhere 2 dimensional, because it is skewed by the centrifugal forces acting on the fluid close to the wall. The flow visualization for the four rows is shown in Fig. 11. No fundamental differences in the behaviour of the boundary layers can be observed. In all cases transition occurs via a separation bubble. The skewing of the boundary layer on the wall can be clearly seen on the rotor blades. It should be noted, that it appears very pronounced on the flow visualization because the density of the liquid dye is higher than that of air.

The applied experimental techniques give a very clear picture of the boundary layer development on the guide vanes. The same behaviour was observed as reported by H.P. Hodson /16/. A large portion of the suction side boundary layer is laminar. Shortly after the velocity peak laminar separation, transition in the free shear layer and reattachment occur. The local differences in the overall turbulence environment, including the periodic wake disturbances do not appear to have significant effects. Within the accuracy of the experiments, no differences among the four rows could be identified.

BOUNDARY LAYER STABILITY

The hot film technique offers the same potential for the investigation of the makrostructure of the boundary layer as the hot wire technique does for free stream turbulence. Fig. 12 presents an analysis of the signal in the time domain for the second guide vane of Fig. 2 as has been reported by J. Hourmouziadis and H.-J. Lichtfuß /17/.

The evolution of the signal fluctuation along the wall measured on the suction side of the second vane in a two stage turbine rig is shown. The probes used have a resolution of approximately 10 kHz. With the passing frequency of the upstream blading at about 5.5 kHz the flow disturbances can not be easily isolated from the overall signal. In the lower part of the oscilloscope pictures the passing frequency has been filtered away. The remaining signal shows the expected evolution of the boundary layer along the profile surface coordinate s.

- Stable laminar flow to rel s = 55.8%
- Increasing instability until laminar separation occurs between 68.8% and 75.3%
- Bursts appearing at 75.3% indicating transition in the separated shear layer
- Strong turbulent reattachment fluctuations at 81.8%
- Low level of disturbances in the turbulent boundary layer at 94.8% which can not be distinguished from that of the laminar flow at 55.8%.

More detailed information can be gained from the analysis of the frequency spectra. A typical example is shown in Fig. 13 for the second guide vane. It can be seen that the periodic fluctuation at the blade passing frequency has a very high RMS value. This observation suggests the separation of the total signal plotted in Fig. 10 into a periodic and a random fluctuation. These diagrams are included in Fig. 13. The surprising result was, that the first peak of the total e/E_0 signal at the laminar separation point was caused by the blade passing frequency alone. The second peak contained practically equal parts from the discrete frequency and the random fluctuation.

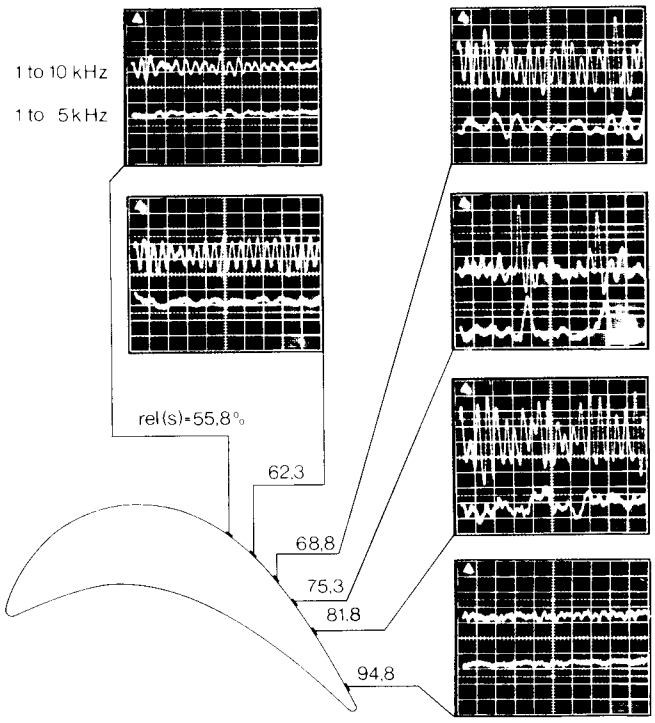

Fig. 12 EVOLUTION OF THE HOT FILM SIGNAL IN THE TIME DOMAIN ON THE SUCTION SIDE OF THE SECOND VANE

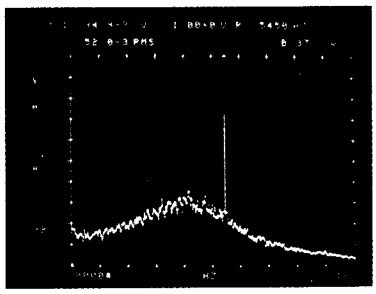

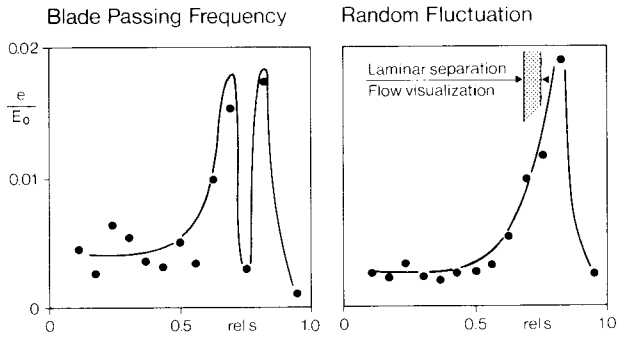

Fig. 13 SEPARATION OF THE RMS HOT FILM SIGNAL INTO A PERIODIC AND A RANDOM FLUCTUATION

Downloaded from http://asmedigitalcollection.asme.org/GT/proceedings-pdf/GT1986/79283/V001T01A107/2396574/v001t01a107-86-gt-244.pdf by guest on 16 August 2022

The evolution of the blade passing frequency amplitude on the suction side is presented in Fig. 14.

- From the leading edge up to the velocity maximum at about rel s = 55% the amplitude is constant and low
- In the diffusing part, the signal is strongly amplified until laminar separation occurs between 68.8% and 75.3%
- Within the laminar separation bubble at 75.3% the disturbance is totally damped down
- In the turbulent reattachment zone at 81.8% the periodic signal is amplified again
- Finally the attached turbulent boundary layer at 94. 8% damps it down to the level of the laminar flow at 55.8%

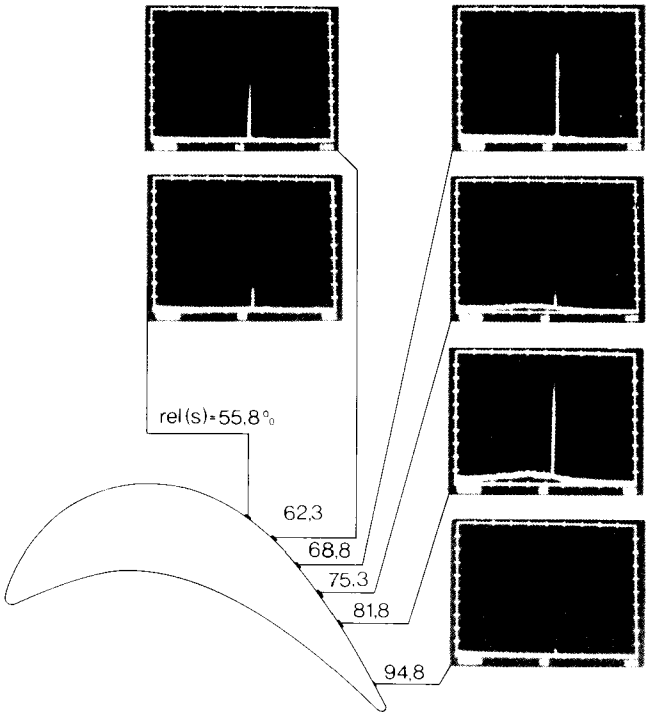

Fig. 14 EVOLUTION OF THE BLADE PASSING FREQUENCY SIGNAL ON THE SUCTION SIDE OF THE SECOND GUIDE VANE

Exactly the same behaviour has also been observed on the first vane, however at significantly lower RMS levels. This is due to the fact that disturbances are not imposed on the boundary layer by the rotor wakes directly, but by the weaker inviscid upstream effects of the rotor flow field, or by acoustic waves.

The development up to the separation point looks very much like the stability behaviour of the laminar boundary layer. It was tried to explain the e/E_0 curve for the blade passing frequency with the linear stability theory developed by W. Tollmien and H. Schlichting /18/. This involves the solution of the Orr-Sommerfeld differential equation. A.R. Wazzan, T.T. Okamura and A.M.O. Smith /19/ have made a parametric study for Hartree velocity profiles. The neutral stability curves they calculated are plotted in Fig. 15. The evolution of the profile boundary layer is shown too. It appears that the laminar profile boundary layer remains deep in the stable region. The alternative possibility was also considered, that these are not weak disturbances, which are amplified moving downstream; but strong disturbances, which are damped down upstream. The Orr-Sommerfeld equation however gives practically 100% damping rates. Obviously linear stability theory does not give an explanation for this phenomenon.

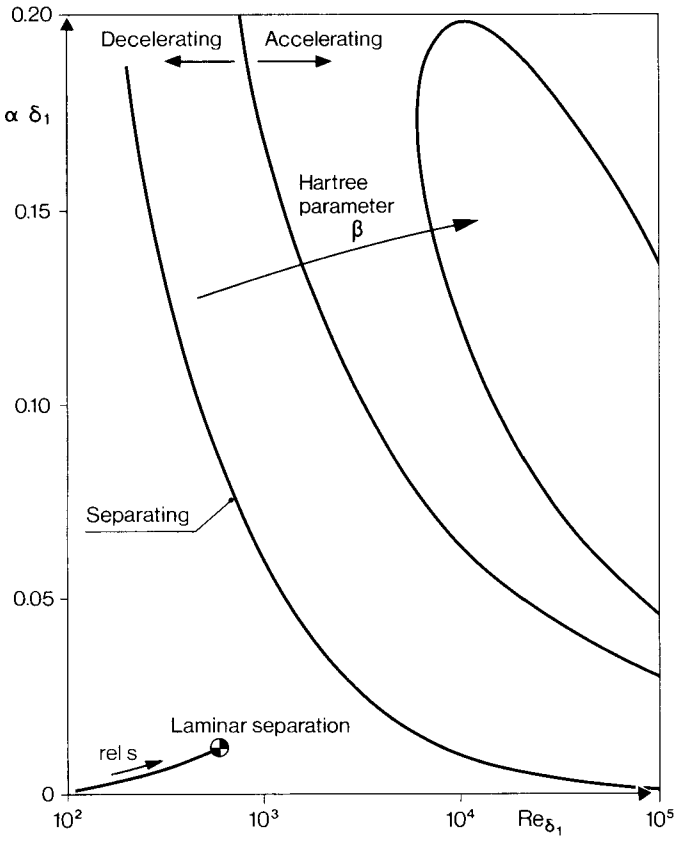

Fig. 15 LAMINAR FLOW NEUTRAL STABILITY CURVES FOR HARTREE PROFILES AND BOUNDARY LAYER EXPERIMENTAL RESULTS

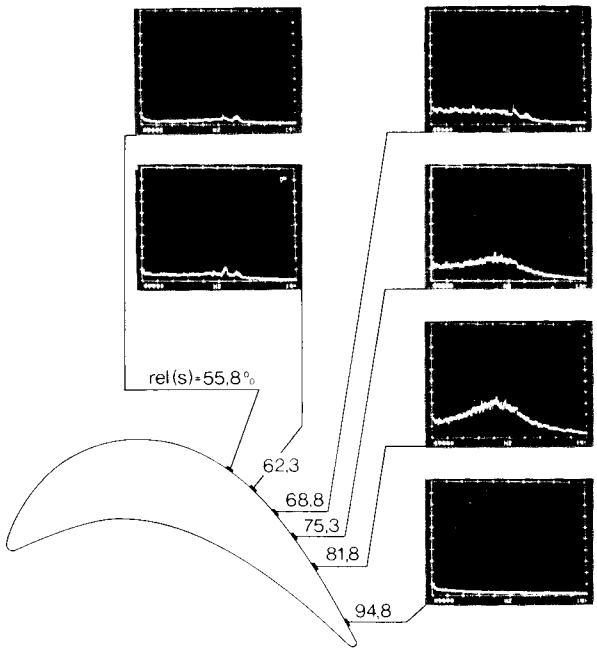

Fig. 16 EVOLUTION OF THE RANDOM FLUCTUATION SIGNAL ON THE SUCTION SIDE OF THE SECOND GUIDE VANE

Downloaded from http://asmedigitalcollection.asme.org/GT/proceedings-pdf/GT1986/79283/V001T01A107/2396574/v001t01a107-86-gt-244.pdf by guest on 16 August 2022

The evolution of the random fluctuation spectrum is shown in Fig. 16.

- From the leading edge to the velocity maximum the amplitude is low and constant over the whole frequency range.
- In the diffusing part, up to the separation point between rel s = 68.8% and 75.3% the signal remains constant over the frequency at increasing levels.
- Within the separation bubble at 75.3% the bursts shown in Fig. 12 lead to a concentration of the fluctuations about 4 kHz.
- In the reattachment region at 81.8% the highest levels of random fluctuations appear contributing to the second peak in Fig. 10. The maximum can still be found at 4 kHz.
- The attached turbulent flow at 94.8% shows only weak and constant fluctuations similar to those of the laminar boundary layer upstream of 55.8%

The last item together with the observations with the blade passing frequency (Fig. 14) and the analysis in the time domain (Fig. 12) indicates that the state of the boundary layer can not be identified from the individual hot film signal. It is necessary to follow the complete development history of the flow.

The amplification of the random fluctuations during deceleration is not as pronounced as the periodic signal was. No selectivity of any particular frequency range can be observed either, as should be expected for stability effects. The high levels at 75.3% and 81.8% are normal for a reattaching turbulent free shear layer. Rearward-facing step experiments performed by D.M. Driver, H.L. Seegmiller and J. Marvin /20/ as well as F.J. Kelly /21/ have shown that the highest levels of turbulence in the flow can be found within the boundary layer at the reattachment point.

At very low frequencies periodic signals from the rotational speed at 39.5 Hz and its higher harmonics were identified on both guide vanes. Fig. 17 shows the spectra in the 0 to 1 kHz range for the second vane. J. Rannacher /22/ has carried out a nonlinear stability analysis accompanied by experiments in a plane boundary layer. He found out that excitation by two different frequencies may lead to periodic fluctuations derived from the difference of those two frequencies. This could be the case with the two rotors of the turbine investigated. However the corresponding value is 3 times 39.5 Hz. Probably it is a combination of this effect with vibrations of the vane itself or acoustic excitation. In any case the hot film signal includes the response of the boundary layer. It can be seen from Fig. 17 that these frequencies are amplified in the same manner random fluctuations are.

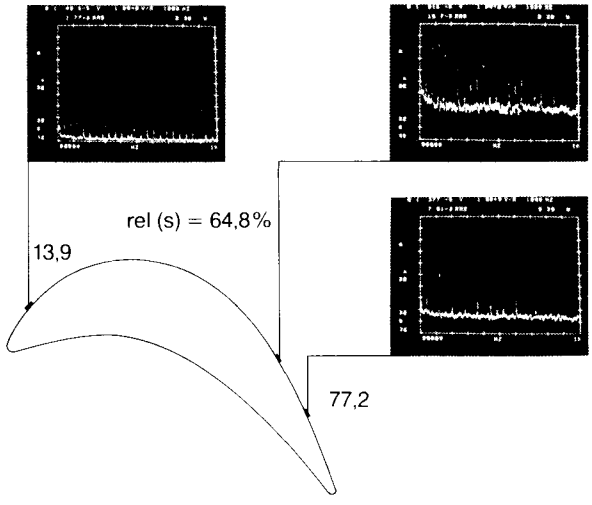

Fig. 17 LOW FREQUENCY PERIODIC FLUCTUATIONS ON THE SUCTION SIDE OF THE SECOND GUIDE VANE

CONCLUSIONS

The experiments on turbulence in turbines show that a large variety of different makrostructures may be present. This includes periodic fluctuations from blade passing frequencies and vortex wakes. The comparison of integral parameters indicates that grid generated turbulence can be made to be very similar to that encountered in a turbine. Periodic disturbances however would have to be introduced separately into the flow.

The experimental techniques applied - profile statics, hot film probes and flow visualization - give a complete understanding of the boundary layer development on the airfoils. The two guide vanes and rotor blades of the two stage rig were exposed to different turbulence environments, particularly in terms of the presence and frequency of rotating upstream wakes. No effects on the fundamental behaviour of the boundary layers could be identified. At all rows transition takes place via a laminar separation bubble.

Both guide vanes showed a very characteristic amplification of the blade passing frequency. The first for the inviscid upstream effects of the rotor flow field, the second for the rotor wakes. These phenomena could not be explained by the linear stability theory of the laminar boundary layer.

It can be concluded that experience from plane cascade tests is a good basis for turbine design. The fundamental boundary layer behaviour in a turbomachinery environment is very similar and can be taken into account with the apropriate prediction techniques available today. It should be noted however that the phenomenon of stability and transition as well as the effects of fluctuating flow in turbomachinery are not yet completely understood. Successful design still relies heavily on calibrating transition criteria from experimental results. A large amount of work is still required to provide the aerodynamicist with the precise tools needed to make the best of a turbine design.

ACKNOWLEDGEMENTS

The authors would like to express their gratitude to Dr.D. Eckardt who originally initiated the investigations. To M. Artmeier, J. Reifenschneider, H. Kneissl and H. Becker from the MTU turbine test group who carried out efficiently the extensive experimental program and the very precise measurements. To Dr.P. Pucher and R. Goehl who developed the hot film technique to a standard that could be used in MTU turbine rigs and evaluated the turbulence and hot film results. Finally to N. Gilbert from the Institut für Theoretische Strömungsmechanik of the DFVLR Göttingen who helped with the solution of the Orr-Sommerfeld equation.

REFERENCES

/1/ J. Surugue, Editor
Boundary Layer Effects in Turbomachines
AGARDograph No. 164, December 1972

/2/ R. Kiock
Boundary Layers on Turbomachinery Blades
Course Note 118, VKI Rhode Saint Genese, February 1983

/3/ D.J. Doorly, M.L.G. Oldfield
Simulation of the Effects of Shock Wave Passing on a Turbine Rotor
ASME 30th IGTC, Houston, 18-21 March 1985, Paper 85-GT-112

/4/ H. Pfeil, R. Herbst
Transition Procedure of Instationary Boundary Layers
ASME, 79-GT-128, 1973

Downloaded from http://asmedigitalcollection.asme.org/GT/proceedings-pdf/GT1986/79283/V001T01A107/2396574/v001t01a107-86-gt-244.pdf by guest on 16 August 2022

/5/ Yu.S. Kachanov, V.Ya. Levchenko
The Resonant Interaction of Disturbances of Laminar-Turbulent Transition in a Boundary Layer
Journal of Fluid Mechanics, January 1984, pp. 209-247

/6/ G.I. Taylor
Some Recent Developments in the Study of Turbulence
Proceedings of the Royal Aeronautical Society, 1936, pp. 294-310

/7/ P. Pucher, R. Goehl
Experimental Investigation of Boundary Layer Separation with Heated Thin-Film Sensors
To be presented at the ASME 31st IGTC, Düsseldorf, June 1986

/8/ O. Lawaczek
Stoß-Grenzschicht-induzierte Ablösung bei transsonischen Turbinengittern
From: Beiträge zur stationären und instationären Aerodynamik, DLR-Forschungsbericht 77/34, 1977

/9/ R. Kiock
Turbulence Downstream of Stationary and Rotating Cascades
ASME Gas Turbine Conference, Washington D.C., 3-12 April 1973, Paper 73-GT-80

/10/ O.P. Sharma, T.L. Butler, H.D. Joslyn, R.P. Dring
An Experimental Investigation of the Three-Dimensional Unsteady Flow in an Axial Flow Turbine
AIAA/SAE/ASME 19th Joint Propulsion Conference, Seattle, 27-29 June 1983, Paper AIAA-83-1170

/11/ R. Kiock
Einfluß des Turbulenzgrades auf die aerodynamischen Eigenschaften von ebenen Verzögerungsgittern
Forschung im Ingenieurwesen, January 1973

/12/ M.F. Blair
Influence of Free-Stream Turbulence on Turbulent Boundary Layer Heat Transfer and Mean Profile Development, Part I -Experimantel Data
Journal of Heat Transfer, February 1983

/13/ R. Kiock, G. Laskowski, H. Hoheisel
Die Erzeugung höherer Turbulenzgrade in der Meßstrecke des Hochgeschwindigkeits-Gitterwindkanals, Braunschweig, zur Simulation turbomaschinenähnlicher Bedingungen
Forschungsbericht, DFVLR-FB 82-25, March 1982

/14/ H.P. Hodson
Boundary Layer and Loss Measurement on the Rotor of an Axial-Flow Turbine
ASME 28th IGTC, Phoenix, Arizona, USA, 27-31 March 1983, Paper 83-GT-4

/15/ H.E. Rohlik, H.W. Allen, H.Z. Herzig
Study of Secondary-Flow Patterns in an Annular Cascade of Turbine Nozzle Blades with Vortex Design
NACA Technical Note 2909, February 1953

/16/ H.P. Hodson
Boundary-Layer Transition and Separation near the Leading Edge of a High-Speed Turbine Blade
ASME 29th IGTC, Amsterdam, 4-7 June 1984, Paper 84-GT-179

/17/ J. Hourmouziadis, H.-J. Lichtfuß
Modern Technology Application to Compressor and Turbine Aerodynamics
7th ISABE, Beijing, 1-4 September 1985

/18/ H. Schlichting
Boundary-Layer Theory
McGraw-Hill Book Co., New York, z. Ed. 1979

/19/ A.R. Wazzan, T.T. Okamura, A.M.O. Smith
Spatial and Temporal Stability Charts for the Falkner-Skan Boundary-Layer Profiles
Douglas Aircraft Company, Report-No. DAC-67086, 1968

/20/ D.M. Driver, H.L. Seegmiller, J. Marvin
Unsteady Behavior of a Reattaching Shear Layer
AIAA 16th Fluid and Plasma Dynamics Conference, Danvers, 12-14 July 1983, Paper AIAA-83-1712

/21/ F.J. Kelly
Turbulent Flow Reattachment - An Experimental Study of the Flow and Structure behind a Backward-Facing Step
Stanford University, Ph.D.Thesis, 1980

/22/ J. Rannacher
Kombinationswirbelfelder in realen Strömungen
ZAMM, 1982, pp. 657-666

Downloaded from http://asmedigitalcollection.asme.org/GT/proceedings-pdf/GT1986/79283/V001T01A107/2396574/v001t01a107-86-gt-244.pdf by guest on 16 August 2022